

Observations and light curve solutions of ultrashort-period eclipsing binaries

Diana P. Kjurkchieva¹, Dinko P. Dimitrov^{2,1}, Sunay I. Ibryamov¹ and Doroteya L. Vasileva^{1*}

¹Department of Physics and Astronomy, Shumen University, 9700 Shumen, Bulgaria

²Institute of Astronomy and NAO, Bulgarian Academy of Sciences

Abstract

Photometric observations in V and I bands and low-dispersion spectra of ten ultrashort-period binaries (NSVS 2175434, NSVS 2607629, NSVS 5038135, NSVS 8040227, NSVS 9747584, NSVS 4876238, ASAS 071829-0336.7, SWASP 074658.62+224448.5, NSVS 2729229, NSVS 10632802) are presented. One of them, NSVS 2729229, is newly discovered target. The results from modeling and analysis of our observations revealed that: (i) Eight targets have overcontact configurations with considerable fillout factor (up to 0.5) while NSVS 4876238 and ASAS 0718-03 have almost contact configurations; (ii) NSVS 4876238 is rare ultrashort-period binary of detached type; (iii) all stellar components are late dwarfs; (iv) the temperature difference of the components of each target does not exceed 400 K; (v) NSVS 2175434 and SWASP 074658.62+224448.5 exhibit total eclipses and their parameters could be assumed as well-determined; (v) NSVS 2729229 shows emission in the $H\alpha$ line. Masses, radii and luminosities of the stellar components were estimated by the empirical relation "period, orbital axis" for short- and ultrashort-period binaries. We found linear relations mass-luminosity and mass-radius for the stellar components of our targets.

Keywords: (stars:) binaries (including multiple): close; (stars:) binaries: eclipsing; stars: late-type; stars: fundamental parameters

1 Introduction

The investigation of short-period contact binary systems is important for the modern astrophysics because they are natural laboratories for study of the late stage of the stellar evolution connected with the processes of mass and angular momentum loss, merging or fusion of the stars (Martin et al. 2011). Moreover, the period-color-luminosity relation makes them useful tracers of distance on small scales (Rucinski 1994; Klagyivik & Csizmadia 2004; Eker et al., 2008).

But the statistics of W UMa stars with short and ultrashort periods ($P \leq 0.23$ d) is relatively poor (Norton et al. 2011, Terrell et al. 2012, Lohr et al. 2013) due to a very sharp decline of the period distribution of binaries with periods below 0.27 days (Drake et al., 2014) as well as faintness of these late stars.

This paper is continuation of our study of ultrashort-period binaries (Dimitrov & Kjurkchieva 2010, 2015, Kjurkchieva et al. 2015, 2016, Kjurkchieva & Dimitrov 2015). It presents results of our photometric and low-resolution spectral observations of ten binaries with orbital periods within 5.1–5.5 hours: NSVS 2175434;

NSVS 2607629; NSVS 5038135; NSVS 8040227; NSVS 9747584; NSVS 4876238; ASAS 071829-0336.7 (further ASAS 0718-03); SWASP 074658.62+224448.5 (further SWASP 0746+22); NSVS 2729229; NSVS 10632802. The targets were selected mainly as a result of searching for short-period eclipsing binaries (Dimitrov 2009) from the NSVS database (Wozniak et al. 2004). Additionally, we included in the sample the known ultrashort-period stars ASAS 0718-03 (Pribulla et al. 2009) and SWASP 0746+22 (Norton et al. 2011) for follow-up observations.

Table 1 presents the coordinates of our targets and available information for their light variability.

2 Observations

Our photometric observations of the targets in V, I bands were carried out in 2010 and 2011 (Table 2) at Rozhen Observatory with the 60-cm Cassegrain telescope using CCD camera FLI PL09000 (3056×3056 pixels, $12 \mu\text{m}/\text{pixel}$) or with 50/70-cm Schmidt telescope equipped by CCD camera FLI PL16803 (4096×4096 pixels, $9 \mu\text{m}/\text{pixel}$). The mean photometric error for each target and each filter are given in Table 3.

*based on observations at NAO Rozhen

Table 1 Preliminary information about the targets

Target	Other name	RA	DEC	mag	Ampl	P	Type	Ref
NSVS 2175434		04 55 22.01	64 53 08.6	13.65(R1)	1.02	0.220951060	EW	1
NSVS 2607629		11 42 25.39	54 52 48.4	12.51(R1)	0.93	0.229370190	EW	1, 13
NSVS 5038135	LINEAR 8209250	13 01 11.06	42 02 12.7	15.34	0.35	0.2254351	EW	3, 4, 12
	1SWASP J130111.22+420214.0							
NSVS 8040227	1SWASP J173003.21+344509.4	17 30 03.06	34 45 02.4	13.78	0.2	0.2237144	EW	3, 4, 8
NSVS 9747584	1SWASP J061850.43+220511.9	06 18 50.43	22 05 11.9	13.87(V)	0.18	0.2143932	EW	2, 3, 4
NSVS 4876238	T-UMa0-03640	09 40 57.29	51 30 39.0	13.76(R)	0.242	0.22183999	EC	11
ASAS 0718-03	V0989 Mon	07 18 28.67	-03 36 39.6	13.75(V)	0.72	0.2112594	EW	5-9
SWASP 0746+22	CRTS J074658.6+224448	07 46 58.62	22 44 48.5	14.27	0.45	0.2208496	EW	3, 4, 8
NSVS 2729229		13 50 06.20	57 26 32.7	14.29		0.22884	new	
NSVS 10632802	LINEAR 15208838	15 39 51.11	10 54 20.4	15.36	0.6	0.2207213	EW	3, 12
	1SWASP J153951.12+105420.7							

Reference: 1 - VSX (Shaw); 2 - Molnar et al. 2013; 3 - Lohr et al. 2013; 4 - Butters et al. 2010; 5 - Kazarovets et al. 2015; 6 - Pribulla et al. 2009; 7 - Pojmanski 2002; 8 - Norton et al. 2011; 9 - Rucinski 2007; 10 - Drake et al. 2014; 11 - Devor et al. 2008; 12 - Palaversa et al. 2013; 13 - Gurol & Michel 2017

The photometric data were reduced in a standard way with the software package MaxImDL by dark subtraction and flat-field division. We performed aperture photometry using more than six comparison stars in the observed field of each target. The photometric data were phased with the periods from Table 1 and the corresponding folded curves are presented in Figs. 1–2. The period of the newly-discovered ultrashort-period binary NSVS 2729229 was determined by the software *PerSea*.

We noted that the amplitudes of half of our light curves differ from the earlier values (Table 1): those of NSVS 2175434 and NSVS 2607629 are smaller while those of NSVS 8040227 and NSVS 9747584 are bigger (Figs. 1–2). The most amazing case is NSVS 2175434 whose amplitude turned out twice smaller than the earlier value.

The low-resolution spectral observations were carried out during 5 nights in 2011 (Table 2) by the 2-m RCC telescope of Rozhen Observatory equipped with focal reducer FoReRo-2 and CCD camera VersArray (512 × 512 pixels, 24 μm/pixel). We used grism with 300 lines/mm that gives resolution 5.223 Å/pixel in the range 5000-7000 Å. The reduction of the spectra was performed with IRAF package by bias subtraction, flat fielding, cosmic ray and nebular lines removal and one-dimensional spectrum extraction. The emission night-sky lines as well as Rb source of emission spectrum were used for wavelength calibration.

The original photometric data and reduced spectra are available at <http://astro.shu.bg/obs-data/10stars/>.

The low-resolution spectra (Fig. 3) do not allow radial velocity measurement and mass ratio determination but are very useful indicators of temperature and stellar activity. All of the objects were spectrally classified by the software package HAMMER of Covey et al. (2007) and the corresponding target temperatures T_m were determined (Table 3). For ASAS 0718-03 we adopted the photometric temperature from Pribulla et al. (2009) determined by its 2MASS color index $J - K$.

Table 2 Journal of the Rozhen observations

Target	Date	Exposure [s]	Telescope
		V, I	
NSVS 2175434	2010 Nov 24	120, 90	60 cm
	2010 Nov 27	120, 120	60 cm
	2011 Jan 17	120, 120	60 cm
	2011 Nov 03	300	2-m
NSVS 2607629	2011 Mar 11	30, 60	60 cm
	2011 Mar 12	30, 60	60 cm
	2011 Mar 13	300	2-m
NSVS 5038135	2011 Mar 14	90, 90	Schmidt
	2011 Apr 11	120, 120	60 cm
	2011 Apr 14	120, 120	60 cm
	2011 Feb 08	300	2-m
NSVS 8040227	2011 Aug 06	120, 120	60 cm
	2011 Aug 07	120, 120	60 cm
	2011 Aug 05	120, 120	60 cm
	2011 Mar 13	300	2-m
NSVS 9747584	2011 Jan 06	120, 120	60 cm
	2011 Jan 07	120, 90	60 cm
	2011 Mar 11	120	2-m
NSVS 4876238	2011 Jan 17	120, 120	60 cm
	2011 Jan 30	120, 120	60 cm
	2011 Mar 11	300	2-m
ASAS 0718-03	2011 Feb 11	120, 120	Schmidt
	2011 Mar 11	120, 120	60 cm
	2011 Mar 12	120, 120	60 cm
SWASP 0746+22	2011 Apr 11	120, 120	60 cm
	2011 Apr 14	120, 120	60 cm
	2011 Mar 12	300	2-m
NSVS 2729229	2011 May 06	120, 120	60 cm
	2011 May 07	120, 120	60 cm
	2011 May 21	120, 120	60 cm
	2011 May 22	120, 120	60 cm
	2011 Mar 12	300	2-m
NSVS 10632802	2011 May 23	120, 120	60 cm
	2011 Mar 13	300	2-m

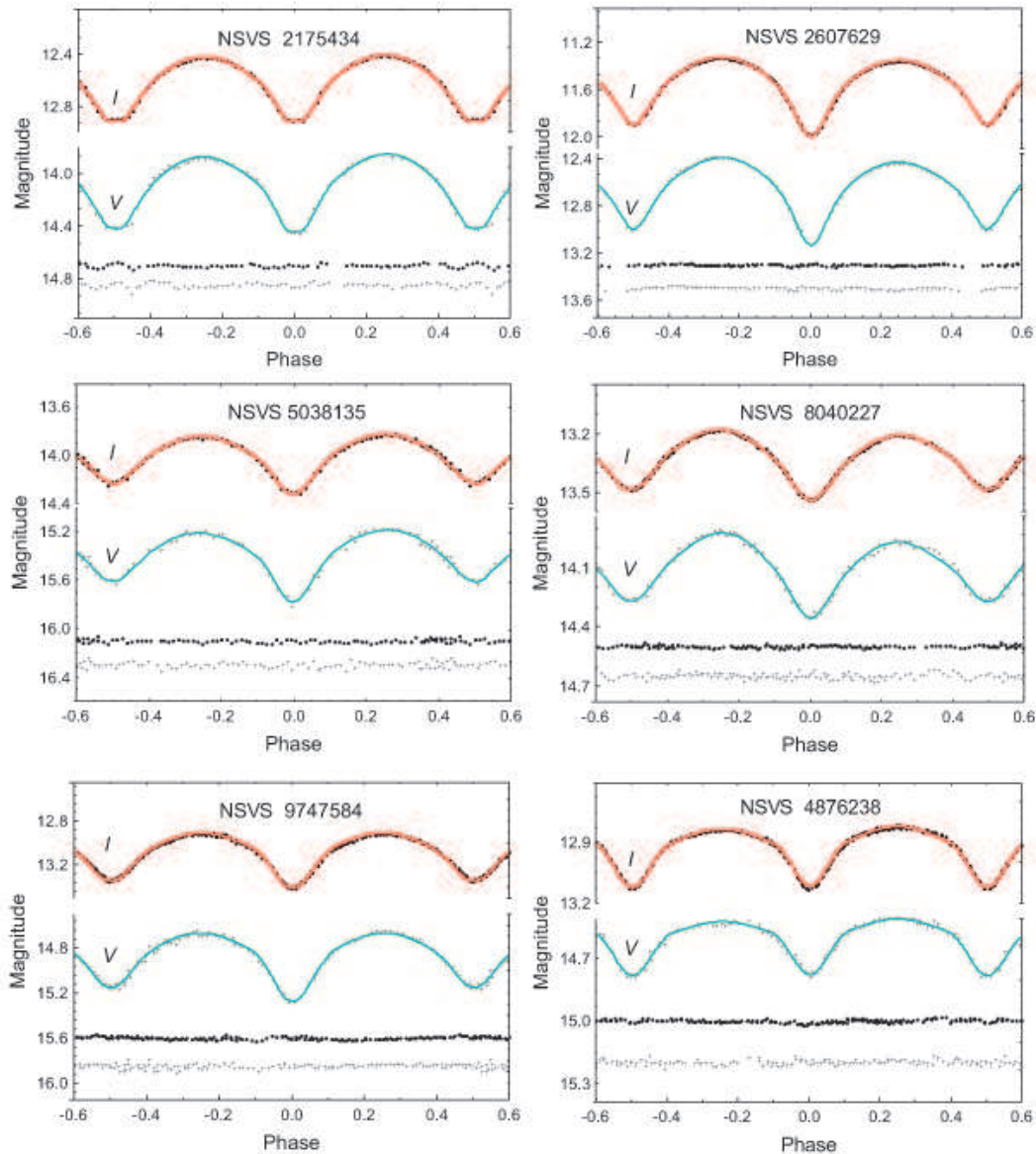
3 Light curve solutions

We carried out the modeling of our data by the package PHOEBE (Prsa & Zwitter 2005) based on the Wilson-Devinney code (Wilson & Devinney 1971).

The procedure of the light curve solutions consists of several steps. Firstly, we adopted primary temperature $T_1 = T_m$ and assumed that the stellar components are MS stars. Then we calculated initial (approximate) values of secondary temperature T_2 , mass ratio q and ratio of relative stellar radii $k = r_2/r_1$, based on the empirical relation of MS stars (Ivanov et al. 2010): $T_2 = T_1(d_2/d_1)^{1/4}$, $q = (T_2/T_1)^{1.6}$, $k = q^{0.75}$.

Table 3 Target spectral type and temperatures T_m , and mean precision σ of our VI photometric observations

Target	NSVS 2175434	NSVS 2607629	NSVS 5038135	NSVS 8040227	NSVS 9747584	NSVS 4876238	ASAS 0718-03	SWASP 0746+22	NSVS 2729229	NSVS 10632802
Sp type	K2	G9	K4	K4	K9	K9	K7	K4	K9	K3
T_m [K]	4900	5300	4600	4600	3850	3850	4000	4600	3850	4750
σ_V [mag]	0.004	0.003	0.006	0.004	0.006	0.005	0.005	0.005	0.005	0.005
σ_I [mag]	0.003	0.002	0.004	0.003	0.003	0.003	0.004	0.003	0.003	0.005


Figure 1. The folded light curves with their fits and the corresponding residuals (shifted vertically by different amount to save space) for the first six targets.

Further we searched for best fit varying: T_2 and q around their initial values; orbital inclination i in the range $60\text{--}90^\circ$ (appropriate for eclipsing stars); potentials $\Omega_{1,2}$ in such way that the ratio r_2/r_1 to correspond to its initial value. We adopted coefficients of gravity bright-

ening 0.32 and reflection effect 0.5 appropriate for late stars (Table 3). The limb-darkening coefficients were chosen according to the tables of Van Hamme (1993). In order to reproduce the light curve distortions we added cool spots on the primary and varied their parameters

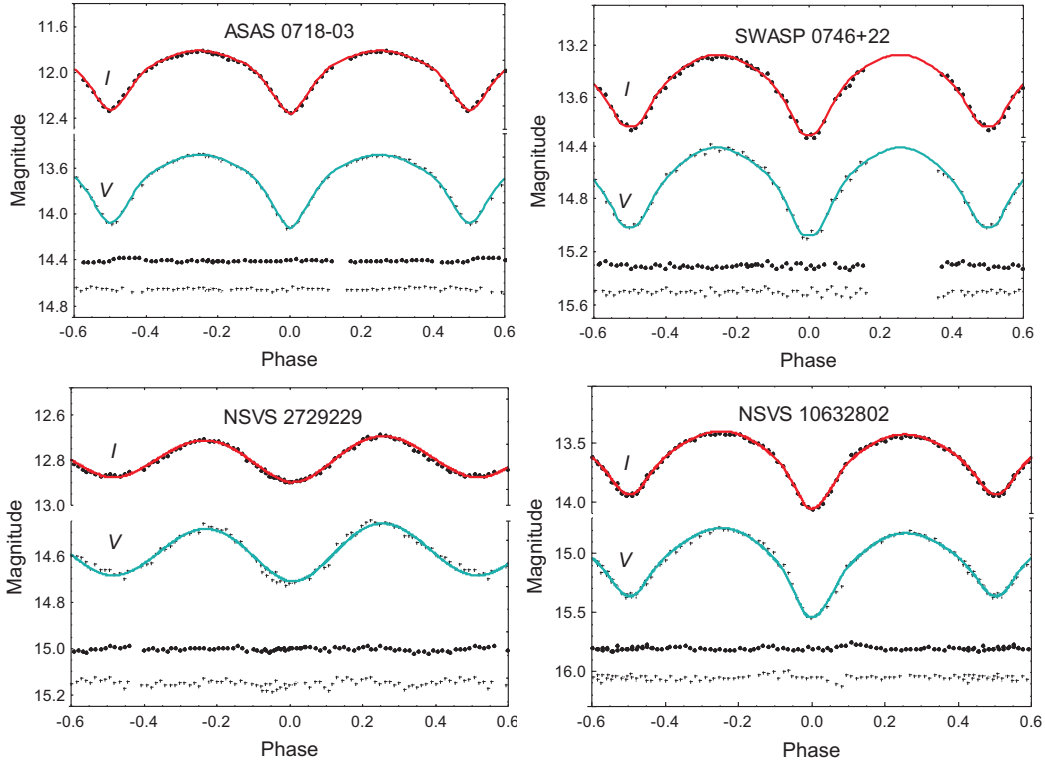


Figure 2. The same as in Figure 1 for the last four targets.

(longitude λ , latitude β , angular size α and temperature factor κ).

After reaching the best solution (corresponding to the minimum of χ^2) we adjusted the stellar temperatures T_1 and T_2 around the value T_m by the formulae (Kjurkchieva & Vasileva 2015)

$$T_1^f = T_m + \frac{c\Delta T}{c+1} \quad (1)$$

$$T_2^f = T_1^f - \Delta T \quad (2)$$

where the quantities $c = L_2/L_1$ (the luminosity ratio of the stellar components) and $\Delta T = T_m - T_2$ are determined from the PHOEBE solution.

The formal PHOEBE errors of the fitted parameters were unreasonably small. That is why we estimated the parameter errors manually by the procedure proposed by Dimitrov et al. (2017). After reaching the best fit the parameter b was changed around its value b^f (corresponding to the best fit) while the rest parameters remained fixed until the biggest deviation of the new synthetic curve from the best-fit synthetic curve became 3σ (σ is the photometric error of the target from Table 3). Then the difference between the new value of b and b^f gives the precision of this parameter. Figure 4

illustrates our method for determination of precision of fitted parameters.

Table 4 contains the final values of the fitted stellar parameters and their uncertainties: initial epoch T_0 ; secondary temperature T_2 ; potentials $\Omega_{1,2}$; inclination i ; mass ratio q and parameters λ and α of equatorial spots with $\kappa = 0.9$. The synthetic curves corresponding to the parameters of our light curve solutions are shown in Figs. 1–2 as continuous lines while Figure 5 exhibits 3D configurations of the targets.

PHOEBE gives a possibility to calculate all values (polar, point, side, and back) of the relative radius $r_i = R_i/a$ of each component (R_i is linear radius and a is orbital separation). Moreover, PHOEBE yields as output parameters bolometric magnitudes M_{bol}^i of the two components in conditional units (when radial velocity data are not available) but their difference $M_{bol}^2 - M_{bol}^1$ determines the true luminosity ratio $c = L_2/L_1$.

Table 5 exhibits the calculated parameters: stellar temperatures $T_{1,2}^f$; relative stellar radii $r_{1,2}$ (back values); ratio of stellar luminosities L_2/L_1 ; fillout factor f . Using the empirical relation P,a for short- and ultrashort-period W UMa type systems (Dimitrov & Kjurkchieva 2015) we calculated target orbital axis a (in solar radii) and thus we were able to estimate masses M_i , radii R_i and luminosities L_i of the stellar compo-

Table 4 Fitted parameters

Star	T_0	T_2	Ω_1	Ω_2	q	i	λ	α
NSVS 2175434	2455579.247328(100)	4895(19)	6.32(4)	6.32(4)	3.01(4)	81.9(1)	90(2)	20(1)
NSVS 2607629	2455632.779863(50)	5090(18)	2.996(2)	2.996(2)	0.619(3)	80.2(1)	270(3)	18(1)
NSVS 5038135	2455663.518774(200)	4449(17)	6.43(2)	6.43(2)	2.96(1)	72.0(1)	90(2)	18(1)
NSVS 8040227	2455780.471376(100)	4356(23)	2.868(4)	2.868(4)	0.522(3)	67.2(1)	270(3)	18(1)
NSVS 9747584	2455568.511660(100)	3741(15)	6.631(8)	6.631(8)	3.091(2)	77.4(1)		
NSVS 4876238	2455579.545545(100)	3816(20)	2.89(1)	2.7(1)	0.379(4)	68.0(1)	90(3)	10(0.5)
ASAS 0718-03	2455604.266489(100)	3942(31)	3.43(1)	3.43(1)	0.83(3)	76.4(1)		
SWASP 0746+22	2455663.304142(100)	4426(32)	6.09(3)	6.09(3)	2.84(3)	81.7(2)		
NSVS 2729229	2455688.551888(400)	3600(20)	3.32(2)	3.32(2)	0.81(1)	49.6(8)	110(2)	16(1)
NSVS 10632802	2455705.435038(200)	4340(20)	5.28(4)	5.28(4)	2.19(1)	79.1(1)	300(3)	25(1)

Table 5 Calculated parameters

Star	T_1^f	T_2^f	r_1	r_2	L_2/L_1	f
NSVS 2175434	4903(20)	4898(19)	0.321(2)	0.507(2)	2.48	0.48
NSVS 2607629	5390(21)	5168(18)	0.445(3)	0.362(3)	0.55	0.28
NSVS 5038135	4704(20)	4553(17)	0.304(1)	0.491(2)	2.23	0.21
NSVS 8040227	4674(26)	4430(23)	0.449(3)	0.336(3)	0.44	0.16
NSVS 9747584	3947(10)	3838(15)	0.297(3)	0.491(3)	8.13	0.17
NSVS 4876238	3860(13)	3826(12)	0.453(1)	0.264(2)	0.45	-0.08
ASAS 0718-03	4025(32)	3967(31)	0.404(2)	0.371(4)	0.78	0.08
SWASP 0746+22	4717(35)	4543(32)	0.327(1)	0.505(2)	2.08	0.51
NSVS 2729229	3942(27)	3692(20)	0.421(3)	0.384(2)	0.59	0.25
NSVS 10632802	4986(28)	4576(20)	0.344(3)	0.479(3)	1.36	0.39

Table 6 Global parameters

Star	a	M_1	M_2	R_1	R_2	L_1	L_2	d [pc]
NSVS 2175434	1.57(5)	0.27(3)	0.81(7)	0.51(2)	0.80(4)	0.131(12)	0.329(41)	398(19)
NSVS 2607629	1.66(5)	0.72(6)	0.45(4)	0.74(3)	0.60(4)	0.412(37)	0.231(30)	283(13)
NSVS 5038135	1.62(5)	0.28(3)	0.84(8)	0.49(2)	0.80(4)	0.106(09)	0.244(30)	759(33)
NSVS 8040227	1.60(5)	0.73(7)	0.38(4)	0.72(3)	0.54(3)	0.222(22)	0.100(14)	364(18)
NSVS 9747584	1.51(5)	0.25(2)	0.76(8)	0.45(2)	0.74(4)	0.044(04)	0.107(14)	261(13)
NSVS 4876238	1.58(5)	0.78(8)	0.30(3)	0.72(2)	0.42(2)	0.102(08)	0.034(04)	237(10)
ASAS 0718-03	1.48(5)	0.53(6)	0.44(4)	0.60(2)	0.55(3)	0.084(09)	0.067(10)	249(13)
SWASP 0746+22	1.57(5)	0.28(3)	0.79(7)	0.52(2)	0.80(4)	0.118(12)	0.241(33)	484(24)
NSVS 2729229	1.65(5)	0.64(6)	0.52(4)	0.70(3)	0.64(4)	0.105(11)	0.067(09)	335(17)
NSVS 10632802	1.57(5)	0.34(3)	0.74(7)	0.54(2)	0.75(4)	0.162(17)	0.223(29)	818(43)

nents in solar units as well as target distance d . Their values are given in Table 6.

4 Analysis of the results and discussion

The main result from the modeling of our photometric and spectral observations of ten ultrashort-period eclipsing binaries is determination of: (i) initial epoch T_0 of all targets; (ii) orbital period of NSVS 2729229; (iii) spectral types and temperatures; (iv) orbital inclination, mass ratio, temperatures and relative radii of stellar components.

The analysis of the obtained parameter values led to the following results.

(1) NSVS 2175434 and SWASP 0746+22 exhibit total eclipses and their photometric mass ratios are reliable (Terrell & Wilson 2005).

(2) Eight targets (NSVS 2175434, NSVS 2607629, NSVS 5038135, NSVS 8040227, NSVS 9747584, SWASP 0746+22, NSVS 2729229, NSVS 10632802) have over-contact configurations (Fig. 5, Table 5) with considerable fillout factor. NSVS 4876238 and ASAS 0718-03 are almost contact configuration (with small fillout factor)

with partial eclipses and their photometric mass ratios are worse determined.

(3) NSVS 4876238 is rare case of detached ultrashort-period binary, similar to BX Tri (Dimitrov & Kjurkchieva 2010) and BW3 V38 (Maceroni & Montalban, 2004).

(4) The temperature differences between the target components are small (up to 400 K) that is expected for overcontact systems. But the almost equal component temperatures of the (slightly) detached binary NSVS 4876238 were not so expected. This result may mean that NSVS 4876238 is a binary oscillating around a marginal-contact state predicted by the thermal relaxation theory (Qian 2002).

(5) All stellar components are K dwarfs excluding the primary of NSVS 2607629 which is slightly hotter star. The components of NSVS 9747584, NSVS 4876238 and NSVS 2729229 are very late K dwarfs (the secondary of NSVS 2729229 is rather M dwarf).

(6) Light curve asymmetries of seven targets were reproduced by cool spots on the side surfaces of their primary components. Surface inhomogeneities are also appearance of stellar activity of late stars.

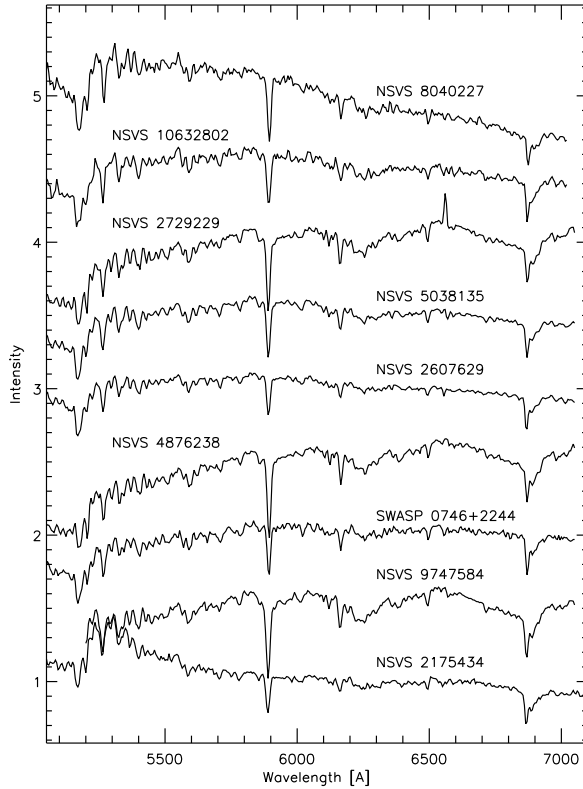


Figure 3. Low-resolution spectra

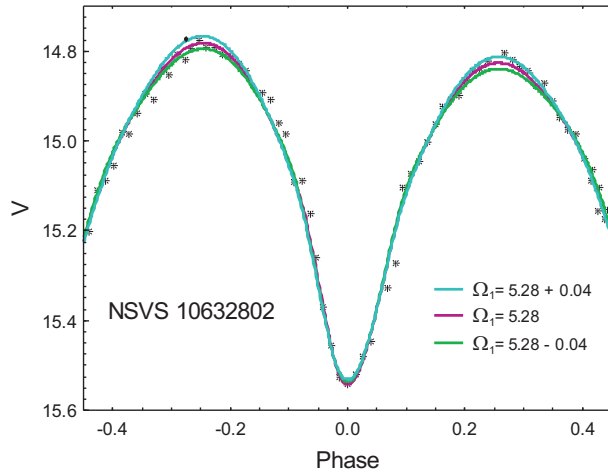


Figure 4. The three synthetic fits used for determination of the precision of Ω_1 of NSVS 10632802

(7) NSVS 2729229 shows emission in H α line (Fig. 3). This is another appearance (besides the spot) of stellar activity of this cool star.

(8) We searched for empirical relations of the global stellar parameters of our ultrashort-period overcontact binaries. It turned out that there is not well-apparent

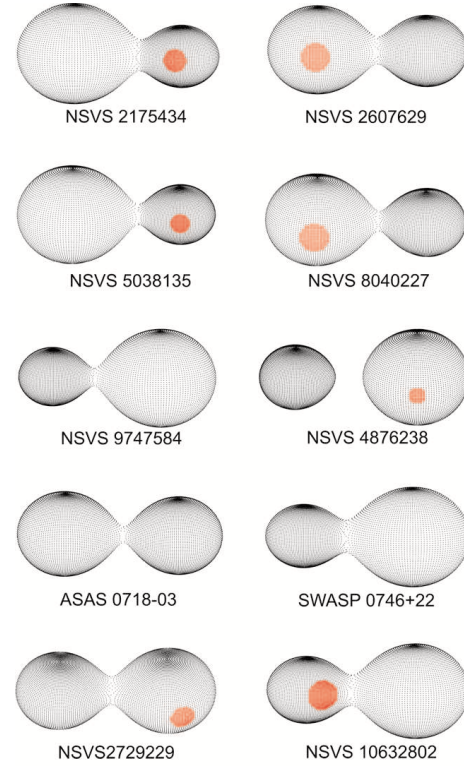


Figure 5. 3D configurations of the targets

relation mass-luminosity (Fig. 5). It may be approximated roughly by the linear function $L \approx 0.32M$. In opposite, the relation mass-radius is quite precise (Fig. 5) and could be described by the linear function $R = 0.33 + 0.55M$.

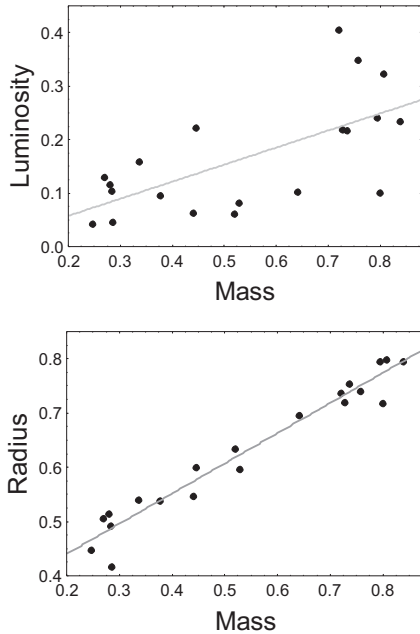
Two of our targets were studied earlier and we present comparison with our results.

(i) Pribulla et al. (2009) carried out *RI* photometric observations of ASAS 0718-03 and obtained estimations of some parameters: mass ratio $q \sim 0.65$; orbital inclination $i \sim 76.8^\circ$; fillout factor $f \sim 0$. For comparison, by detailed light curve solution of our *VI* data we obtained for the same parameters: $q = 0.83$; $i = 76.4^\circ$; $f = 0.08$. The different values of mass ratio support insensitivity of the light curve solutions of the partially-eclipsed binaries to this parameter.

(ii) Based on *BVR_c* light curves and their modeling Gurol & Michel (2017) obtained parameters of NSVS 2607629 (first row of Table 7). The comparison with our values (second row of Table 7) illustrates the duplicity of the solutions of overcontact systems: A-subtype configuration corresponding to $q^{(1)} < 1$ and $r_1^{(1)} > r_2^{(1)}$ and W-subtype configuration corresponding to $q^{(2)} \approx 1/q^{(1)} > 1$, $r_1^{(2)} \approx r_2^{(1)}$ and $r_2^{(2)} \approx r_1^{(1)}$. The supposition about such W/A ambiguity was made firstly by van Hamme (1982) and Lapasset & Claria (1986) who noted that

Table 7 Two sets of parameters of NSVS 2607629

Source	T_1 [K]	T_2 [K]	q	i [$^\circ$]	r_1	r_2	M_1 [M_\odot]	M_2 [M_\odot]	R_1 [R_\odot]	R_2 [R_\odot]	L_1 [L_\odot]	L_2 [L_\odot]	f	d [pc]	α [$^\circ$]
G&M	5420	5110	1.65	77.7	0.37	0.46	0.44	0.73	0.57	0.71	0.25	0.31	0.07	144	18
our	5390	5168	0.62	80.2	0.45	0.36	0.72	0.45	0.74	0.60	0.41	0.22	0.28	255	59


Figure 6. Relations mass-luminosity and mass-radius for the target components

sometimes both A and W configurations can fit well the photometric observations and the right choice between the two solutions requires spectral mass ratio.

Another difference between the two solutions of NSVS 2607629 was that Gurol & Michel (2017) used a large hot spot on the secondary component while we obtained considerably smaller cool spot on the primary. Although the two solutions reproduce the same effect (the light at the first quadrature to be smaller than that at the second quadrature, true for the two runs of observations, in March 2011 and in March 2016) we assume that cool spots are physically more reasonable for late stars. This result illustrates another ambiguity of the light curve solution: hot spot on the primary has the same effect as appropriate cool spot on the secondary and viceversa.

Conclusion

We presented photometric and low-resolution spectral observations of ten ultrashort-period eclipsing binaries. The target temperatures were determined by their spectral type while the orbital inclination and mass ratio as

well as relative radii and temperatures of stellar components were derived from the light curve solutions. The stellar masses, radii and luminosities were estimated by the empirical relation for short- and ultrashort-period binaries.

This study enriches the poor statistics of ultrashort-period binaries with known parameters and improved our understanding of these late stars. Target NSVS 2729229 from our sample of ten ultrashort-period binaries is newly-discovered member of this family.

Acknowledgements

This study is supported by projects DN 08-20/2016, DN 08-1/2016 and DM 08-02/2016 of National Science Foundation of Bulgarian Ministry of education and science as well as by projects RD 08-102 and RD 08-80 of Shumen University. The authors are very grateful to the anonymous referee for the valuable recommendations and notes.

This research makes use of the SIMBAD database, VizieR service, and Aladin previewer operated at CDS, Strasbourg, France, and NASA's Astrophysics Data System Abstract Service.

REFERENCES

- Butters O.W. et al., 2010, *A & A* 520, L10
 Covey K.R. et al., 2007, *AJ*, 134, 2398
 Devor J. et al., 2008, *AJ*, 135, 850
 Dimitrov D.P., 2009, *BlgAJ*, 12, 49
 Dimitrov D.P., Kjurkchieva D.P., 2010, *MNRAS*, 406, 2559
 Dimitrov D.P., Kjurkchieva D.P., 2015, *MNRAS*, 448, 2890
 Dimitrov D.P., Kjurkchieva D.P., Iliev I. Kh., 2017, *MNRAS*, 469, 2089
 Drake A. et al., 2014, *ApJS*, 213, 9
 Eker Z., Demircan O., Bilir S., 2008, *MNRAS*, 386, 1756
 Gurol B., Michel R., 2017, *NewA*, 51, 128
 Ivanov V.P., Kjurkchieva D.P., M. Srinivasa Rao, 2010, *BASI*, 38, 83
 Kazarovets E.V., Samus N.N., Durlevich O.V., Kireeva N.N., Pastukhova E.N., 2015, *IBVS* 6151
 Kjurkchieva D., Dimitrov D., Ibryamov S., 2015, *RAA*, 15, 1493
 Kjurkchieva D.P., Dimitrov D.P., 2015, *AN*, 336, 153
 Kjurkchieva, D., Vasileva, 2015, *PASA*, 32, 23
 Kjurkchieva D., Popov V., Vasileva D., Petrov N., 2016, *SerAJ*, 192, 21

- Klagyivik P., Csizmadia S. 2004, Publications of the Astronomy Department of the Eotvos Lorand University, 14, 303
- Lapasset E., Claria J.J., 1986, A & A, 161, 264
- Lohr M. et al., 2013, A & A, 549A, 86
- Martin E.L., Spruit H.C., Tata R. 2011, A & A, 535, A50
- Molnar L.A. et al., 2013, arXiv:1310.0539
- Norton A. et al., 2011, A & A, 528A, 90
- Palaversa L. et al., 2013, AJ, 146, 101
- Pojmanski G., 2002, Acta Astronomica, 52, 397
- Pribulla T., Vanko M., Hambalek L., 2009, IBVS 5886
- Prsa A., Zwitter T., 2005, ApJ, 628, 426
- Qian S., 2002, MNRAS, 336, 1247
- Rucinski S., 1994, PASP, 106, 462
- Rucinski S., 2007, MNRAS, 382, 393
- Rucinski S., 2009, MNRAS, 382, 393
- Rucinski S., Pribulla T., 2009, MNRAS, 382, 393
- Terrell D., Gross J., Cooney W., 2012, AJ, 143, 99
- Van Hamme, W., 1982, A & A, 105, 389
- Van Hamme, W., 1993, AJ, 106, 2096
- Wilson R.E., Devinney E.J., 1971, ApJ, 166, 605